



Fire-Induced Thermal Fields in Window Glass. II—Experiments

A. A. Joshi* & P. J. Pagni

Mechanical Engineering Department, University of California at Berkeley, Berkeley,
California 94720, USA

(Received 5 November 1992; revised version received 21 April 1993,
accepted 10 May 1993)

ABSTRACT

The authors' previously presented model determines the time to breakage of window glass exposed to a compartment fire. The physical and mechanical properties of glass and the history of the compartment fire are required. Among the mechanical properties of glass, the breaking stress, σ_b , is the least well known. Here, experiments on 59 plate glass samples using the four-point flexure method are described to determine the breaking stress distribution. This distribution is described by a three-parameter cumulative Weibull function, $G(\sigma_b) = 0$, for $\sigma_b < \sigma_u$ and

$$G(\sigma_b) = 1 - \exp\left(-\left(\frac{\sigma_b - \sigma_u}{\sigma_0}\right)^m\right) \quad \text{for } \sigma_b \geq \sigma_u$$

with the parameters $m = 1.21$, $\sigma_0 = 33$ MPa and $\sigma_u = 35.8$ MPa. A breaking stress of 40 MPa (5800 psi) was determined to be a reasonable value to use in breaking calculations for ordinary window glass. The breaking patterns of the test specimens suggest that fractures initiate at edge imperfections rather than at surface flaws. Some experiments to estimate the heat transfer coefficient inside the compartment and the emissivity of the hot layer are also described and values are suggested for use in the model.

NOTATION

- a Distance between points of load application in flexure test
 b Width of the glass specimen

* Present address: Mechanical Engineering Department, University of California, Santa Barbara, California 93106, USA.

c	Distance between supports in flexure test
E	Young's modulus
g	Weibull distribution function
G	Cumulative Weibull distribution function
h	Heat transfer coefficient
k	Thermal conductivity
l	Decay length
L	Thickness of the glass sample
m	Exponent in Weibull distribution function
N	Number of specimen
P	Breaking load
Q	Energy
s	Shaded length
T	Temperature
u	Dummy variable
V	Volume
α	Thermal diffusivity
β	Thermal expansion coefficient
ϵ	Emissivity
θ	Dimensionless temperature
τ	Dimensionless time
ξ	Dimensionless x coordinate
σ	Stress

Subscripts

1	Ambient side of glass pane
2	Compartment side of glass pane
b	breakage
c	Characteristic
i	Initial
r	Radiation
s	Stored in glass
y	Diffusion in shaded portion
∞	Ambient

1 INTRODUCTION

A theoretical model has been presented¹ which incorporates the energy exchanges between the fire, the window and the ambient, in order to predict the time to and temperature at breakage of glass windows exposed to fires. This model uses the following parameters: (1) thermo-physical and mechanical properties of glass; (2) the outer

ambient and inner hot gas temperature; (3) the heat transfer coefficient at the outer and inner glass surfaces; and (4) flame radiation from the fire, in order to calculate the temperature histories of the glass surfaces.

The physical properties of the particular glass in question and the ambient temperature at the outer surface can be determined quite accurately by standard measurement techniques. The heat transfer coefficient at the outer glass surface can also be estimated to a reasonable accuracy. The hot gas temperature and the flame radiation for a particular compartment fire can be obtained by using a fire simulation technique, for example, FIRST.² Among the mechanical properties, the Young's modulus and the thermal coefficient of expansion can be determined quite accurately.

The estimation of remaining quantities, that is, the breaking stress of glass, the heat transfer coefficient at the inner surface and emissivity of the hot layer, is more difficult and is the goal of this paper. In Section 2, the procedure for estimating the breaking stress of ordinary window glass is discussed. The experiments conducted for estimating the breaking stress are described and statistical analysis of the results is presented. In Section 3, results from some compartment fire experiments are given. While direct measurements are not made, the values of the heat transfer coefficient at the inner glass surface and the emissivity of the hot layer which provide agreement with these data are estimated.

2 BREAKING STRESS OF ORDINARY WINDOW GLASS

Glass is a well studied brittle material and yet there is significant uncertainty in determining its strength.³ The mechanical properties of glass are similar to those of a crystalline solid. Below the breaking limit, glass is elastic and returns to its original shape after the release of forces that cause its deformation. The failure of glass is usually from tension.

Glass strength depends strongly upon the treatment and handling of its surface.³ Tiny flaws or cracks on the glass surface lead to weakening and failure by brittle fracture. There is also a 'size effect' on strength.⁴ As the specimen size is decreased, the average stress at fracture tends to increase. These observations may be explained by noting that all real materials invariably contain a distribution of flaws of varying severity such as surface scratches and cracks at grain boundaries. If the material behavior is predominantly elastic, the high local stresses around such flaws cannot be relieved appreciably by plastic deformation as they could be if ductile behavior occurred. Since larger specimens can

contain more flaws than smaller specimens, the probability of a more severe flaw existing in a brittle material such as glass is higher for a larger specimen.

By assuming a flaw of a given geometry, and knowing the fracture toughness values, estimates may be made for the flaw sizes which are responsible for the observed tensile strength values of glass. However, it is observed that in materials such as glass and graphite the typical flaws are too small to be detected by a microscope of resolution $0.1 \mu\text{m}$.⁴ Thus, due to the uncertainties involved, a probabilistic rather than a deterministic approach is needed.

Tensile strength tests are carried out on a number of nearly identical specimens to obtain a distribution of breaking stress values. The usual procedure for tensile strength determination of materials is to hold the sample between two jaws and subject it to uniaxial tension. For a brittle material like glass, however, the usual tensile test is not conducted, as there is a possibility of breakage at the grips. Hence, a flexure method is normally used.⁴ A four-point flexure method is used here since, in the large area between the two points of load application, there is a uniform bending moment which also corresponds to the maximum stress. Since in most cases breakage occurs in the area of maximum stress, the four-point method gives a good estimate of the breaking stress.

To quantify statistically the uncertainty in the breaking strength of glass, it has been shown that the Weibull probability distribution successfully represents the glass breaking stress data.⁵ In this paper, the two- and three-parameter Weibull distribution functions are discussed. The results, along with an error analysis, of a four-point flexure experiment on ordinary window glass samples ($178 \text{ mm} \times 25.4 \text{ mm} \times 2.5 \text{ mm}$) are presented. The experimental set-up is described and the statistical analysis of the results to fit the Weibull distribution⁶ is conducted. Schematics of broken glass beams for different load ranges are also included to show the breaking patterns corresponding to different energy storage levels.

2.1 Experiments

An Instron Universal Testing Instrument was used to determine the tensile strength of the glass specimens. This instrument incorporates a highly sensitive weighing system with load cells that use strain gages for detecting and recording tensile or compressive load. An applied load on the cell causes a proportional change in the resistance of the strain

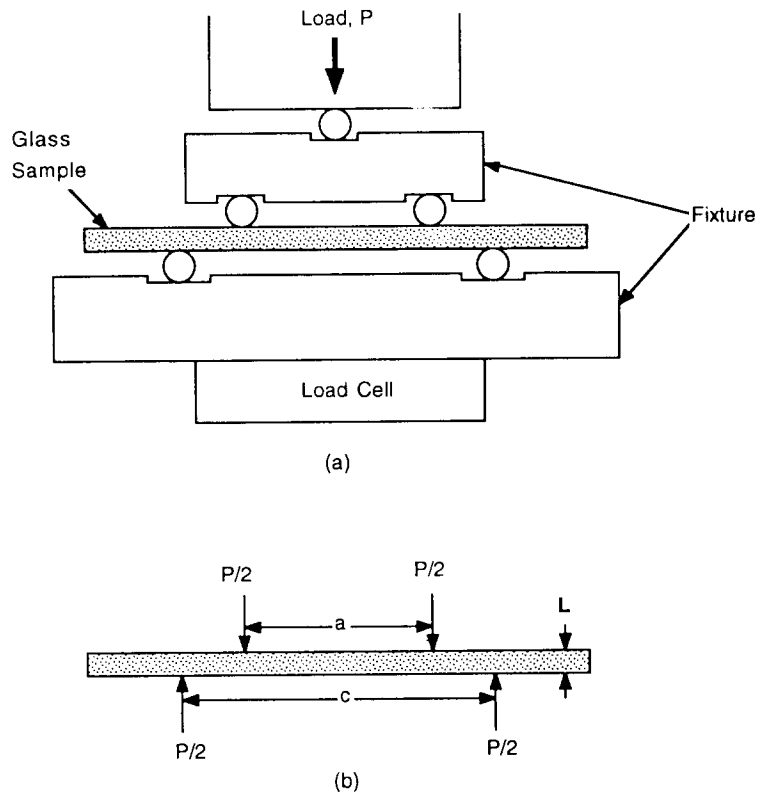


Fig. 1. Schematic diagram of the experimental set-up. Here, $c = 132$ mm and $a = 38.6$ mm.

gages. These gages are arranged in a bridge circuit and excited by a stabilized oscillator. The resulting signal is amplified, rectified to d.c. and fed to the pen driving circuit of a null-balance, high speed recorder. The amplifier circuit also incorporates flexible means for balancing the load cell to compensate for varying weights of jaws, fixtures and the samples themselves.

A fixture with the sample was placed on the load cell of the instrument to provide a four-point load on the glass beam as shown in Fig. 1. The sample is thus in contact with two rollers on top of which an increasing load was applied from the Instron instrument. The magnitude of the load was detected by the strain gages in the load cell which transmitted that information to the strip chart recorder. Loading was stopped when the glass beam broke. Fifty-nine samples were tested and the results are explained below.

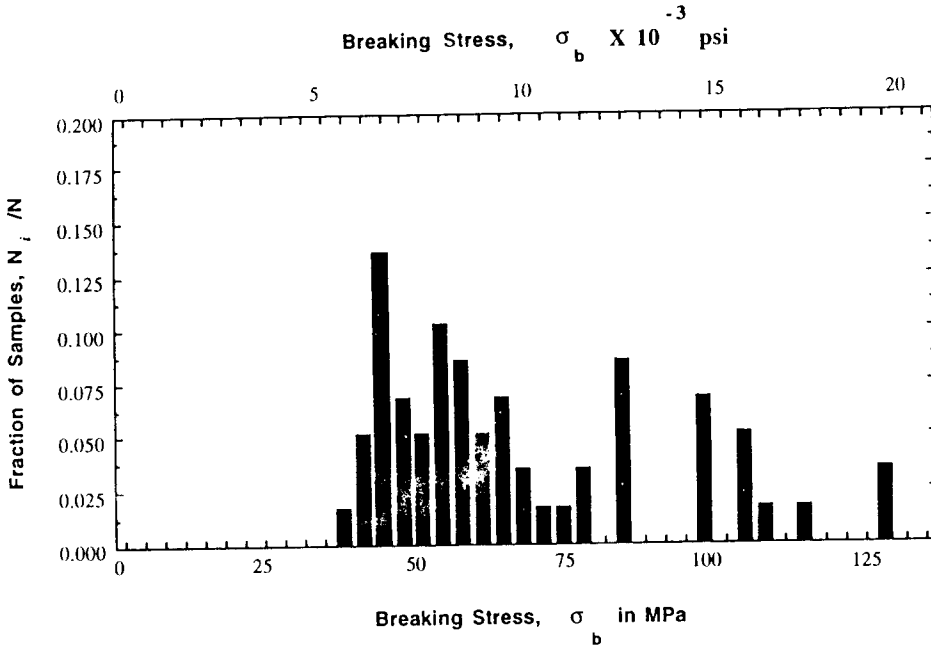


Fig. 2. Histogram of the breaking stress of the 59 samples $178 \text{ mm} \times 25.4 \text{ mm} \times 2.5 \text{ mm}$. The strength of majority of the samples is between 41 and 45 MPa.

2.2 Results

From elementary beam theory,⁷ the maximum stress for this four-point load configuration is:

$$\sigma_b = \frac{3P(c-a)}{2bL^2} \quad (1)$$

Here, σ_b is the breaking stress; P is the breaking load; c is the distance between the two sample supports; a is the distance between the two points of load application; b is the width, and L is the specimen thickness. This formula was used to estimate the breaking stress.

Figure 2 shows a histogram of the breaking strength of the 59 samples. A large variation in breaking stress with a minimum value of 36.8 MPa and the maximum value of 128 MPa can be clearly seen. The high value of breaking stress is possibly due to the absence of severe edge flaws on such a small-sized sample.

The largest fractional squared error in determining the breaking stress of glass using eqn (1) is:

$$\left(\frac{\Delta\sigma_b}{\sigma_b}\right)^2 = \left(\frac{\Delta P}{P}\right)^2 + \left(\frac{\Delta c}{c-a}\right)^2 + \left(\frac{\Delta a}{c-a}\right)^2 + \left(\frac{\Delta b}{b}\right)^2 + 4\left(\frac{\Delta L}{L}\right)^2 \quad (2)$$

Here, $P_{\min} = 36.5$ N, $P_{\max} = 137$ N, $c - a = 92.7$ mm, $b = 25.2$ mm, and $L = 2.3$ mm. The least counts on the various instruments used were: $\Delta P = 0.88$ N, $\Delta b = \Delta L = 0.025$ mm, and $\Delta c = \Delta a = 1.3$ mm, which gives:

$$\left. \frac{\Delta \sigma_b}{\sigma_b} \right|_{\min} = 0.03; \quad \left. \frac{\Delta \sigma_b}{\sigma_b} \right|_{\min} = 0.04 \quad (3)$$

Thus, the experimental error in the breaking stress measurement decreases from 4% to 3% as P increases over the range from 36.5 to 137 N. Since this error is much smaller than the measured breaking stress range, the distribution resulting from these measurements is realistic.

Figure 3(a) shows the schematic of a glass beam, sample no. 34, which broke at a relatively low load ($P = 37.4$ N, $\sigma_b = 38$ MPa). Only one smooth fracture exists. The reason for a single crack is that a low load corresponds to a low elastic energy and so fewer bonds are broken in the glass. Figure 3(b) is the schematic of a glass beam (sample no. 39) which broke at an intermediate load ($P = 55.6$ N, $\sigma_b = 57$ MPa). Three main pieces of the glass are seen. As the elastic energy associated with

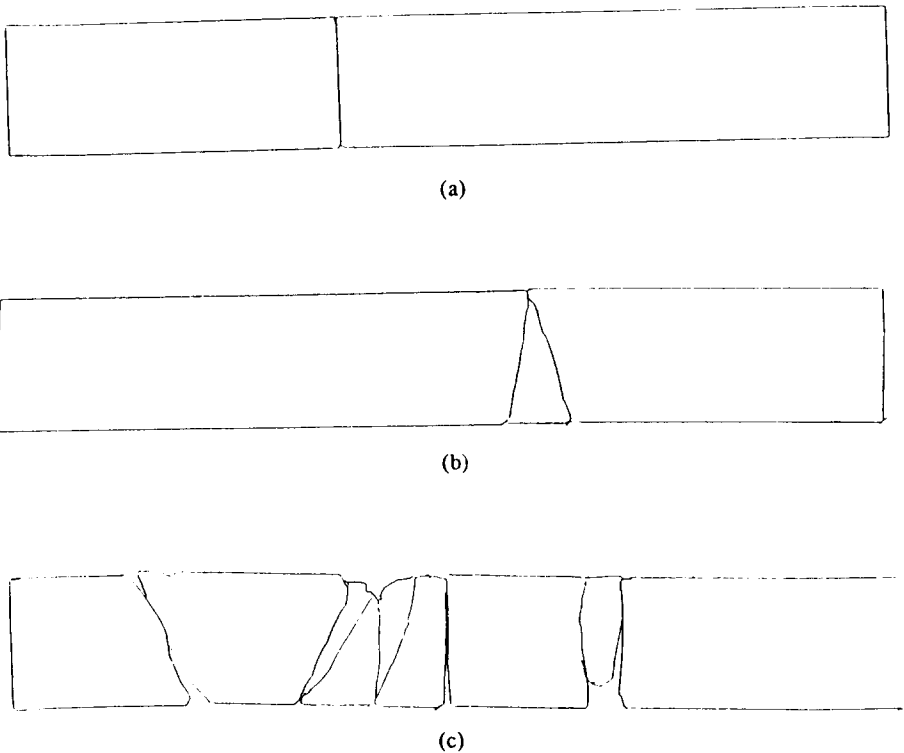


Fig. 3. Breaking pattern schematics of samples at different loads. (a) Load = 37.4 N, $\sigma_b = 38$ MPa; (b) load = 55.6 N, $\sigma_b = 57$ MPa; (c) load = 137 N, $\sigma_b = 128$ MPa.

this load is increased, more bonds are broken. Figure 3(c) is a schematic of a glass beam (sample no. 18) which broke at a high load ($P = 137$ N, $\sigma_b = 128$ MPa). The glass has broken into many pieces, due to the large amount of elastic energy stored prior to breakage. Observation of the cross-section of a glass beam breaking at a low load showed that the fracture was conchoidal and originated at an edge. It would appear to be a safe assumption that all fractures obtained in these experiments were edge originated.

2.3 Weibull distribution parameters

When a large number of specimens are tested and a histogram of the breaking stress, σ_b , is obtained for small intervals, a continuous curve can be drawn as shown in Fig. 4(a). Then, by scaling the ordinate such that the area under this curve is unity, the probability density function $g(\sigma_b)$ is obtained as shown in Fig. 4(b). The density function, $g(\sigma_b)$, shows the relative frequency with which different values of strength are observed. The shaded area in Fig. 4(b) represents the probability that a specimen will have a strength between zero and infinity. Then, the probability, $G(\sigma_b)$, that a specimen will fail at a stress level less than or equal to σ_b is the area under the $g(\sigma_b)$ curve from zero to σ_b . Thus, the cumulative distribution function, $G(\sigma_b)$, shown schematically in Fig. 4(c) and which will be used here, is given by:

$$G(\sigma_b) = \int_0^{\sigma_b} g(\sigma') d\sigma' \quad (4)$$

The general form of the cumulative Weibull distribution function is:

$$G(\sigma_b) = 1 - e^{-\int \phi(\sigma_b) dV/V_0} \quad (5)$$

where σ_b is the breaking stress; ϕ is some function of σ_b ; V is the volume (or area) of the sample; and V_0 is some characteristic volume (or area). Weibull⁶ arrived at this formula by applying a series model to the flaws. The series model⁴ simply states that the strength of the sample is the strength of the weakest unit making up the sample. Weibull⁶ initially chose $\phi(\sigma_b) = (\sigma_b/\sigma_0)^m$ as a simple empirical expression which fitted experimental data representing the breaking stress of glass as a Weibull function. The parameters which characterize the two-parameter Weibull distribution function are m and σ_0 .

A limitation of the simple two-parameter Weibull distribution is that

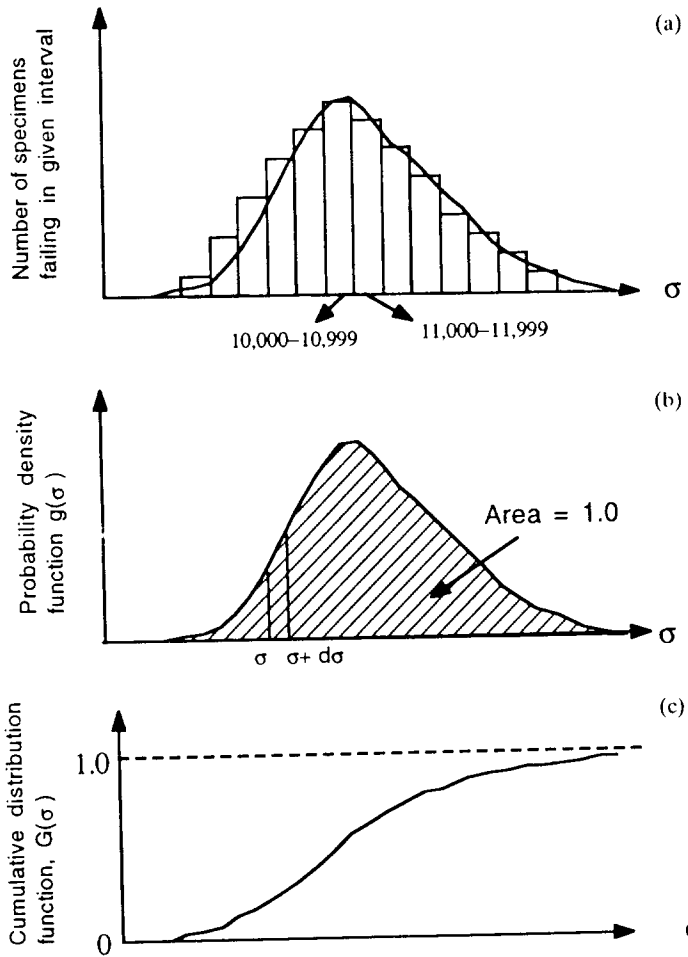


Fig. 4. (a) Schematic histogram of breaking stress. (b) Schematic probability density function evaluated from the histogram of Fig. 4(a). (c) Schematic cumulative distribution function evaluated from Fig. 4(b).

it predicts a small but finite probability of failure at low stresses. To provide a more realistic distribution, Weibull⁶ proposed a three-parameter distribution with $\phi(\sigma_b) = [(\sigma_b - \sigma_u)/\sigma_0]^m$:

$$G(\sigma_b) = 1 - e^{-\int(\sigma_b - \sigma_u/\sigma_0)^m dV/V_0}, \quad \sigma_b > \sigma_u \quad (6)$$

$$0, \quad \sigma_b \leq \sigma_u$$

The additional parameter, σ_u , is often referred to as the zero strength or the lowest strength of specimens of size V . The parameters m , σ_0 and σ_u are obtained by fitting the experimentally obtained values of breaking stress to the Weibull functions as explained below. It is

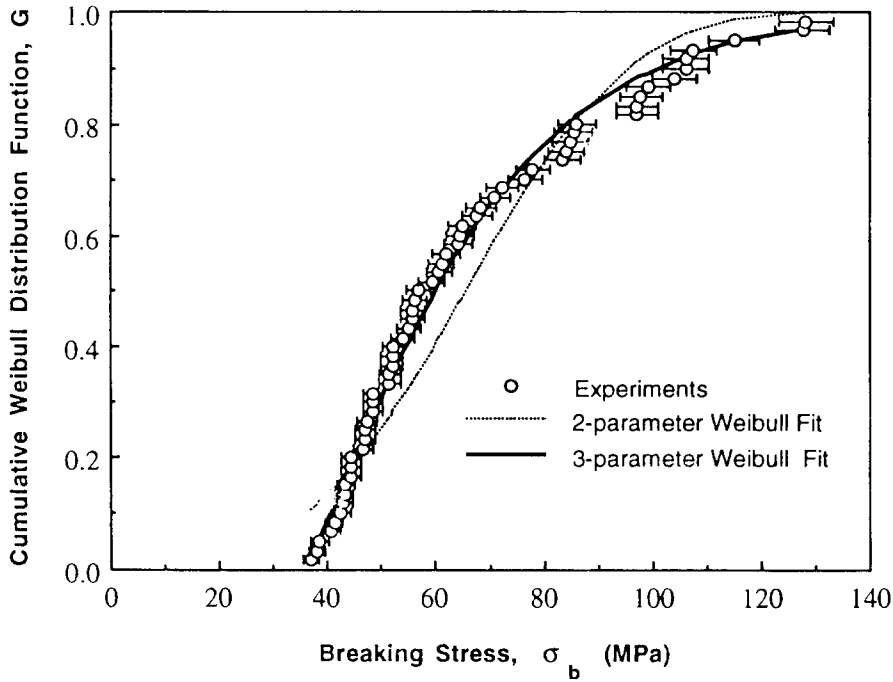


Fig. 5. Cumulative distribution function of the experimental breaking stress along with the two- and three-parameter Weibull functions. The three-parameter Weibull distribution function shown here is clearly a good fit. The error bars indicate the 3–4% experimental error.

assumed here that the breaking stresses do not depend on the volume and V_0 is assumed to be equal to the total volume of the specimen. This eliminates the integral in eqn (6) to give the three-parameter distribution stated in the abstract.

The values of strength obtained from all the N observations are arranged in an increasing order $j = 1, 2 \dots N$, where $\sigma_{b_j} \geq \sigma_{b_{j-1}}$. Since there are a limited number of observations, it is practical to plot the cumulative distribution function, $G(\sigma_b)$, directly as a function of σ_b , as shown in Fig. 5. The ordinate, however, cannot be simply j/N as that would imply that the strongest, corresponding to a probability of 1, of all possible specimens was present in the limited samplings. Expressions such as:

$$G(\sigma_b) = j/(N + 1) \quad (7)$$

or:

$$G(\sigma_b) = (j - 0.3)/(N + 0.4) \quad (8)$$

are commonly used⁶ which do not indicate that either the strongest or

weakest of all possible specimens were present in the sampling. The first is the mean value of probability corresponding to the j th observation. The second expression is a close approximation to median plotting position, that is, half of the j th observations are above and half are below σ_b . Here, the mean rank is chosen so that $G = j/(N + 1)$.

For a specimen volume V in the case of pure tension, or specimen area V in the case of uniform tension in flexure, the value of m is obtained as follows. Taking the logarithm of eqn (5) for the two-parameter function assuming no volumetric dependence gives:

$$\ln \frac{1}{1-G} = (\sigma_b/\sigma_0)^m V/V_0 \quad (9)$$

Substituting eqn (7) for G and taking the logarithm once again gives:

$$\ln \ln \left(\frac{N+1}{N+1-j} \right) = m \ln \sigma_b - m \ln \sigma_0 + \ln V - \ln V_0 \quad (10)$$

Thus, the slope of a plot of $\ln \ln [(N + 1)/(N + 1 - j)]$ versus $\ln \sigma_b$ is equal to m . For the three-parameter distribution, the term $m \ln \sigma_b$ is replaced by $m \ln (\sigma_b - \sigma_u)$. Since σ_u is not known, trial values are chosen and the one for which a plot of $\ln \ln [(N + 1)/(N + 1 - j)]$ versus $\ln (\sigma_b - \sigma_u)$ best fits a straight line is selected.

From a plot for the two-parameter Weibull distribution for our samples, the values of m obtained was 3.20 and the value of σ_0 obtained was 74.1 MPa with $V = V_0$. The coefficient of determination⁸ for this fit was 0.86 indicating that the fit is reasonable as shown in Fig. 5. For the three-parameter Weibull distribution, the value of σ_u which gave the best fit was 35.8 MPa. The value of m obtained from this plot was 1.21; the value of σ_0 was 33.0 MPa with $V = V_0$. Here the coefficient of determination was 0.99, a much better fit as indicated in any other experimental data for comparison. Figure 5 shows a plot of $G(\sigma_b)$ versus σ_b for the experiments along with error bars and two- and three-parameter Weibull fits for the parameters given in Table 1. From the three-parameter Weibull distribution function, it is clear that a

TABLE 1
Parameters for Two- and Three-Parameter Weibull Distribution Functions

Weibull function	m	σ_0 (MPa)	σ_u (MPa)
Two-parameter	3.20	74.1	—
Three-parameter	1.21	33.0	35.8

value of 40 MPa for σ_b , would be conservative estimate and is recommended for calculations.

3 GLASS HEATING EXPERIMENTS IN COMPARTMENT FIRES

In this section, the results of experiments on glass breaking in compartment fires conducted at the Virginia Polytechnic Institute and State University⁹ are evaluated and the variation of the heat transfer coefficient at the inner glass surface, h_2 , and the emissivity of the hot gas layer, ϵ_{2s} , are estimated. Some compartment fire experiments at the University of California Richmond Field Station are also described.¹⁰

3.1 Experiments at the Virginia polytechnic Institute and State University

In this experimental study,⁹ liquid hexane, contained in pans of different sizes, was ignited in the center of a compartment of dimensions 1.52 m \times 1.22 m \times 0.99 m. This compartment had a 0.36 m \times 0.56 m aluminum frame on one of the walls, in which a 0.28 m \times 0.51 m glass window of thickness 2.4 mm was installed. The glass was cut by hand with a scribe and the edges were not ground in any way. The pan sizes, 0.3 m \times 0.2 m, 0.2 m \times 0.2 m and 0.2 m (diameter) were much smaller than the compartment size. Since the fire was small, heating of the window was slow and was dominated by convection from hot upper layer gases. Higher than actual temperatures may have been read by the thermocouples on the glass because of radiative heating.

Glass breakage times were reported for two sets of experiments. In the first set, the window had shaded edges. The insulation used was 9.5-mm-wide cellular rubber weather stripping. The window was held in place against the weather stripping by metal washers. In these experiments, the time history of the temperatures at the central inner surface and on the shaded edges of the glass and the breakage time were recorded for different pan fires. The gas temperature was not measured. In the second set, the windows were held fixed by reversible washers against the frame and did not have shaded edges; the windows were fully exposed to the fires. Only the gas temperature and the temperature of the inner glass surface were measured as a function of time in the second set.

Since there was no run in which the gas and glass temperatures and the breaking time were given for the same fire, exact comparisons are

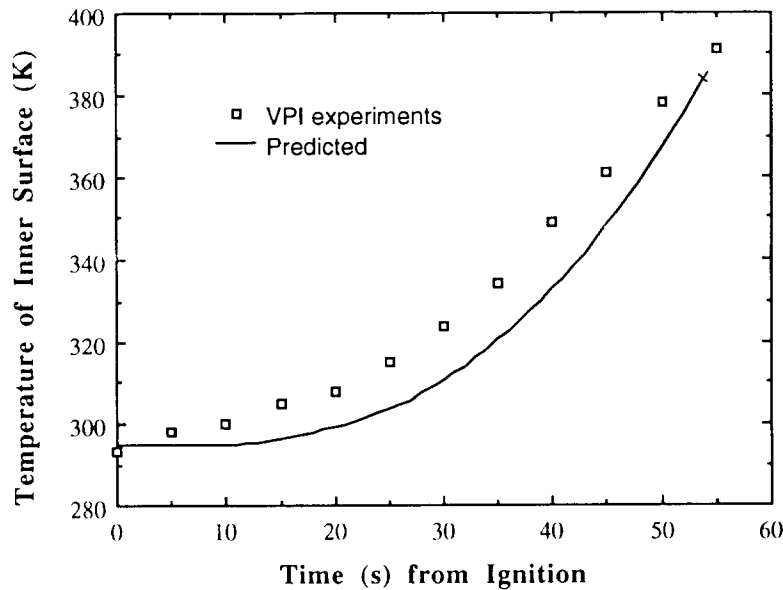


Fig. 6a. Comparison of experimental⁹ inner glass surface temperature with the predicted values for a 0.3 m × 0.2 m pan fire (test no. 1). The last experimental point and the cross on the theoretical prediction indicate breakage.

not possible. However, the hot layer temperature histories arising from fires in pans of same size are expected to be similar. Using average gas temperatures calculated from their data for pan fires of same sizes in BREAK,¹¹ variations of h_2 and ϵ_{2x} were chosen for which the breaking times matched. The radiative flux function, $j(\tau)$, was set equal to zero since the pan fires were small. The material properties used in the calculations⁹ were $\sigma_b = 47$ MPa, $\beta = 3.6 \times 10^{-6} \text{ K}^{-1}$ and $E = 70$ GPa. The heat transfer coefficient on the outside, h_1 , was set equal to $10 \text{ W/m}^2\text{-K}$, $k = 0.76 \text{ W/m-K}$, $\alpha = 3.6 \times 10^{-7} \text{ m}^2/\text{s}$ and $l = 1$ mm. The other inputs used here were $L = 2.4$ mm, $s = 9.5$ mm and $H = 0.14$ m.

Figures 6a and 6b show the comparisons of the experimental and predicted inner glass surface temperatures for a 0.3 m × 0.2 m pan fire and a 0.2 m × 0.2 m pan fire, respectively. The experimental values of the temperatures were higher (~10%) probably due to the absorption of radiation by the thermocouples. For 0.3 m × 0.2 m pan fires, the reported breaking times were 55, 56 and 48 s. Taking $h_2 = 10 \text{ W/m}^2\text{-K}$ at $t = 0$ and increasing linearly with time to $40 \text{ W/m}^2\text{-K}$ at $t = 60$ s and emissivity, ϵ_{2x} , as 0.1 at $t = 0$ and also increasing linearly to 0.9 at $t = 100$ s for the same size pan fire, the breaking time predicted by BREAK1 is 54 s which gives good agreement with the experimental average of 53 s. At that time, the average dimensionless surface

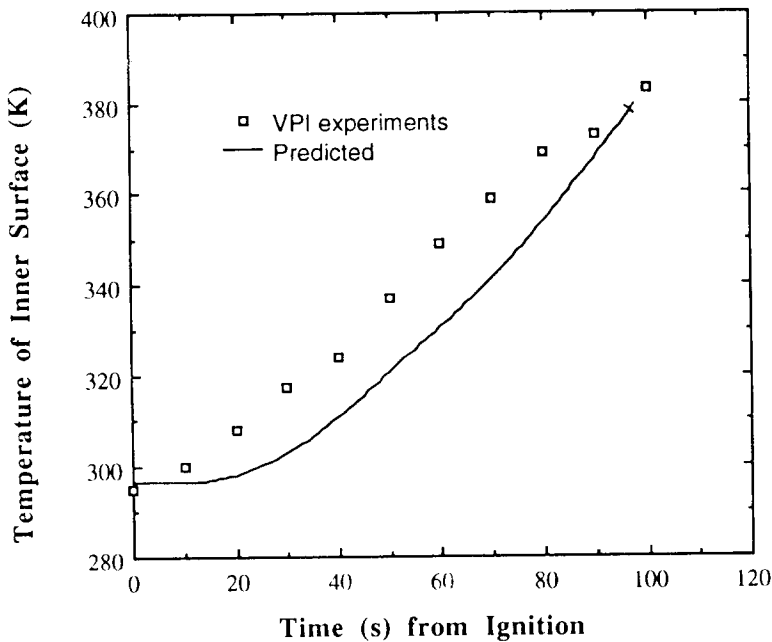


Fig. 6b. Comparison of experimental inner glass surface temperature with the predicted values for a $0.2\text{ m} \times 0.2\text{ m}$ pan fire (test no. 4). The last experimental point and the cross on the theoretical prediction indicate breakage.

temperature $\bar{\theta} = 1.04$, the dimensionless breaking time $\tau_b = 3.38$, the hot gas temperature $T_{2\infty} = 720\text{ K}$, the heat transfer coefficient of the hot side $h_2 = 37\text{ W/m}^2\text{-K}$, and the emissivity of the hot gas $\varepsilon_{2\infty} = 0.6$. For the 0.2 m square pan fires, the reported breaking times were 100, 112 and 109 s. Taking h_2 as $10\text{ W/m}^2\text{-K}$ at $t = 0$ and again increasing linearly to $40\text{ W/m}^2\text{-K}$ at 200 s and $\varepsilon_{2\infty}$ as 0.1 at $t = 0$ and increasing linearly to 0.9 at $t = 500\text{ s}$, gives a predicted breaking time of 96 s in reasonable agreement with the experimental average of 107 s. At this time, $\bar{\theta} = 1.05$, $\tau_b = 6.06$, $T_{2\infty} = 651\text{ K}$, $h_2 = 24\text{ W/m}^2\text{-K}$ and $\varepsilon_{2\infty} = 0.18$. Figures 7a and 7b show the heat flow and energy storage histories for the experiments described in Figs 6a and 6b, respectively.

The choice of a linear ramp for h_2 and $\varepsilon_{2\infty}$ was made considering that at $t = 0$ the heat transfer to the glass is by natural convection of cooler gases, while at longer times, as the gas temperature increases, the heat transfer is by turbulent convection forced by the fire plume. The emissivity of the hot layer is low at early time because the hot layer thickness is small. The emissivity increases with time because of increased soot, products and pyrolyzates in the hot layer. The agreement between the experimental and predicted time to breakage is good

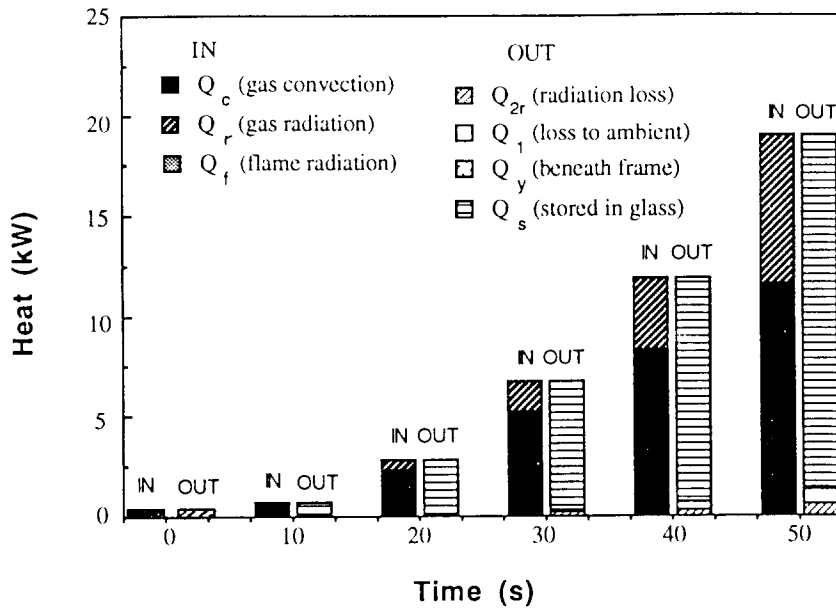


Fig. 7a. Predicted evolution of the magnitudes of the various energy flow and storage terms for the 0.3 m x 0.2 m, Virginia Polytechnic Institute (VPI) compartment pan fire shown in Fig. 6a.

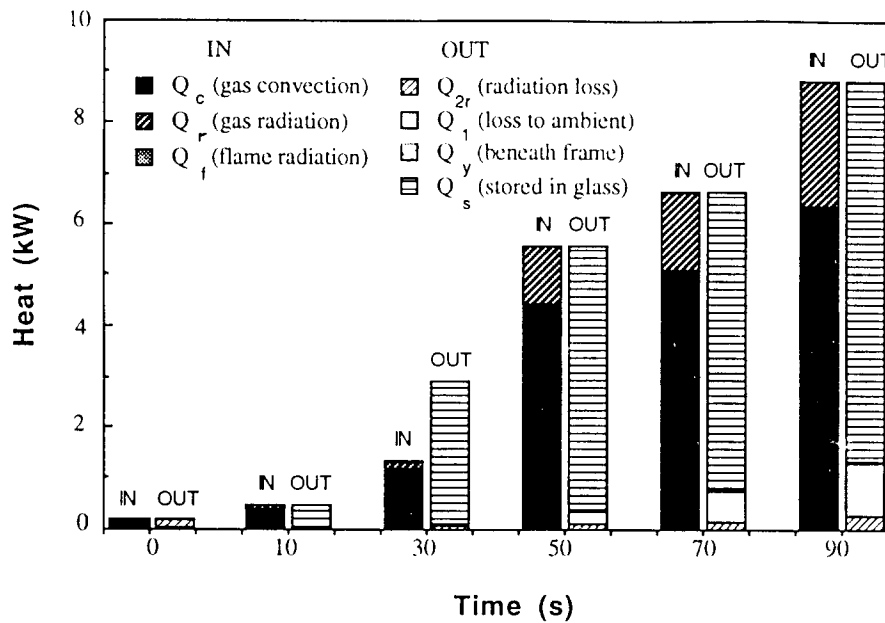


Fig. 7b. Predicted evolution of the magnitudes of the various energy flow and storage terms for the 0.2 m x 0.2 m, Virginia Polytechnic Institute (VPI) compartment pan fire shown in Fig. 6b.

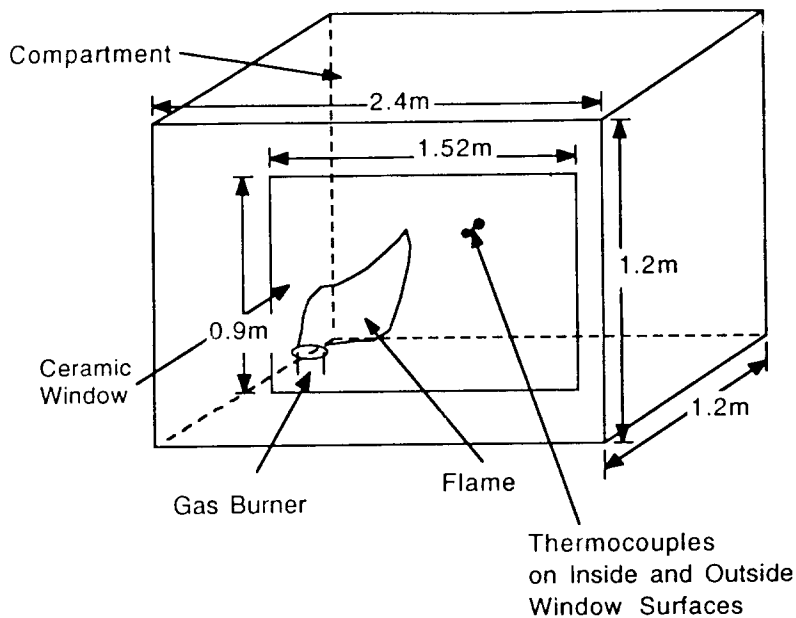


Fig. 8. Schematic diagram of the experimental backdraft chamber in the Fire Research Laboratory at the Richmond Field Station of the University of California at Berkeley, described in Ref. 10.

for both pan fires for the chosen variations of the heat transfer coefficient and emissivity of hot layer. Similar variations are used to compare glass temperatures in the next section.

3.2 Experiments at the University of California Richmond Field Station

Additional experiments were performed in a test chamber designed by Fleischmann¹⁰ and used for backdraft experiments. Figure 8 shows the schematic diagram of the experimental chamber. The internal dimensions of the test chamber were 1.2 m wide, 1.2 m high and 2.4 m long. The walls were constructed with two layers of 16 mm Type X, fire rated, gypsum wall board to provide structural strength and 51 mm refractory fiber blanket for fire resistance.

Due to the explosive nature of backdrafts, one of the 1.2 m \times 2.4 m walls was hinged at the bottom and made to open to relieve pressure greater than 965 Pa. In the other 1.2 m \times 2.4 m wall, a 0.9-m-high and 1.5-m-wide window was installed. The glass in the observation window was made of Neoceram,¹² a clear ceramic with a negative expansion coefficient at low temperatures enabling it to resist temperatures up to

800 °C. Using a heat resistant glass rather than ordinary window glass should not affect the heat transfer coefficient. Knowledge of the glass surface temperature history then allows estimation of the heat transfer coefficient in the fire environment.

The glass surface temperatures were measured by K-type Chromel-Alumel 'Stikon' thermocouples made from 0.25 mm Teflon covered leads. Other thermocouples were also attached to the glass with Omega CC high temperature sodium silicate cement. The gas temperatures were measured by the K-type thermocouples made from 0.5 mm chromel-alumel thermocouple wire. An Autodata Ten/5 Calculating Data Acquisition System was used with the thermocouples. It is a medium speed, high resolution data acquisition system designed for use in harsh or laboratory environments. Signal input modules of this system accept direct inputs from thermocouples.

The experiments were conducted using a 0.3 m square sand burner with natural gas as fuel. The chamber was filled with fuel at a gas flow rate corresponding to an energy release rate of approximately 150 kW. A small vent, 25 mm high by 300 mm long was placed in one 1.2 m × 1.2 m wall near the floor to allow a little ventilation to mimic leakage in full-scale compartments. The fuel was ignited with a spark. The constant fuel flow was shut off after 3 min.

An initial attempt at finding $h_2(t)$ is shown in Fig. 9a. It is clear that the thermocouple supposedly measuring the inner glass surface temperature tracks the gas temperature quite closely. There is also a significant temperature difference between inner and outer surfaces. In two other experiments, similar results were obtained. Using the gas temperature variation as an input field and other parameters $L = 6.3$ mm, $h_1 = 10$ W/m²-K, $k = 1.37$ W/m-K, $\alpha = 6.87 \times 10^{-7}$ m²/s, $l = 1$ mm, $\sigma_b = 392$ MPa, $E = 68.6$ GPa and $\beta = 3.6 \times 10^{-7}$ K⁻¹ as inputs to BREAK1,¹¹ the algorithm for window glass breaking in compartment fires, the value of h_2 is estimated. For these experiments, an unrealistically high value for h_2 , of the order of 1000 W/m²-K, was required to get agreement between the calculated and the apparent measured value of the inner surface temperature. The outer glass surface temperature agreement was poor. This led to the conclusion that the glass thermocouple was probably detached and not detecting the surface temperature but rather was reading the gas temperature. The 'Stikon' thermocouples, applied to the glass surface, had an operating range of -73 to 260 °C. Since the measured gas temperatures were higher than that limit, the cement failed to keep the thermocouple attached to the glass surface. Omega CC sodium silicate cement with a capability of resisting as high as 830 °C was later used but it fused with the glass,

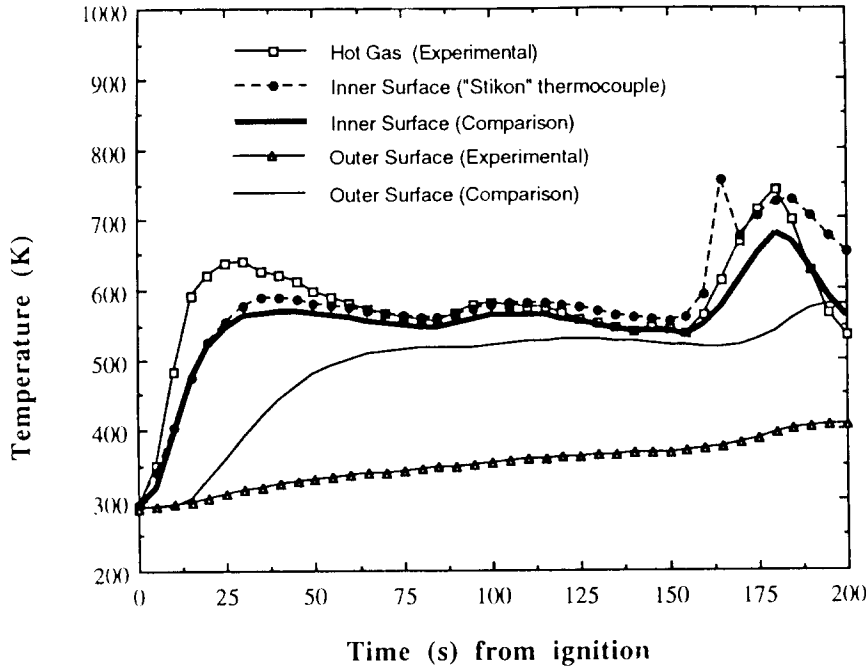


Fig. 9a. Experimental histories of the hot layer temperature, the 'Stikon' thermocouple temperature and the outer glass temperature¹⁰ and predicted values of the inner and outer surface temperatures, using an unrealistically high h_2 in an attempt to match the 'Stikon' thermocouple as if it were the glass inner surface temperature. The peak at ~ 3 min is the backdraft.

causing small pieces of glass to adhere to the cement when the glass cooled which came off during cleaning, thus leaving chips in the glass surface.

However, using the variation of h_2 and ε_{2x} estimated from the Virginia Polytechnic Institute experiments, with the gas temperatures measured in these experiments, the temperature of the outer glass surface could be predicted and compared with data. Figure 9b shows the comparison for one experiment, along with the predicted inner surface glass temperatures. Here, as in Section 3.1, h_2 is assumed to be $10 \text{ W/m}^2\text{-K}$ at $t=0$ and to rise linearly to $40 \text{ W/m}^2\text{-K}$ at 60 s. The emissivity of the hot layer, ε_{2x} , was assumed to be 0.1 at $t=0$ and to rise linearly to 0.9 at 240 s. The agreement between the experimental and predicted outer surface temperatures is good. Figure 9c shows the heat flow and energy storage histories for the experiment described in Figs 9a and 9b. The oxygen in the compartment is sufficiently depleted within 60 s to effectively extinguish the flame, creating the unusual decrease in the energy storage rate.

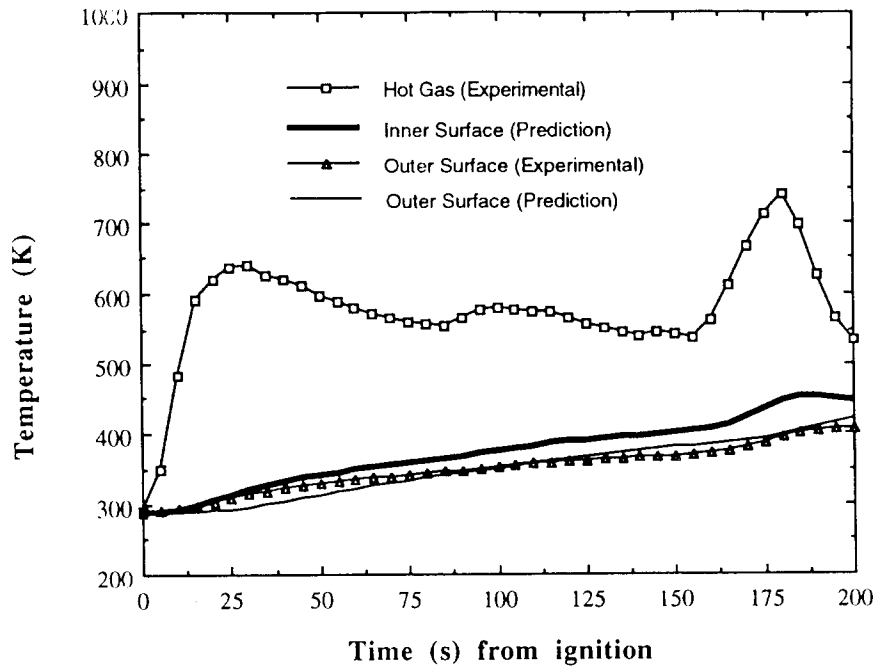


Fig. 9b. Experimental histories of the hot layer temperature and the glass outer temperature¹⁰ and predicted values of the inner and outer surface temperatures using the same linear ramps for h_2 and $\varepsilon_{2\%}$ as in the Virginia Polytechnic Institute (VPI) experiments.

4 CONCLUSIONS

To estimate the breaking stress of ordinary window glass, the distribution of the breaking stress of glass beams ($1/8 \text{ mm} \times 25.4 \text{ mm} \times 2.5 \text{ mm}$) is determined using the four-point-bending method. The results indicate that there is a large variation in the breaking strength of glass of nearly identical specimens. The lowest value observed for breaking stress is 36.5 MPa and the highest value is 128 MPa. The breaking stress distribution is well represented by a three-parameter Weibull distribution with $m = 1.21$, $\sigma_0 = 32.9 \text{ MPa}$ and $\sigma_u = 35.8 \text{ MPa}$.

Different patterns are observed for glass breaking at different loads: glass samples with a higher strength broke into many small pieces due to the elastic energy associated with the higher breaking stress ($\sigma_b > 100 \text{ MPa}$), while lower load ($\sigma_b < 40 \text{ MPa}$) samples broke clearly in a single fracture. Observation of the cross-sections of the broken specimens indicates that in most samples, the fracture initiates at an edge and is conchoidal in nature.

The heat transfer coefficient at the inner glass surface, h_2 , and the

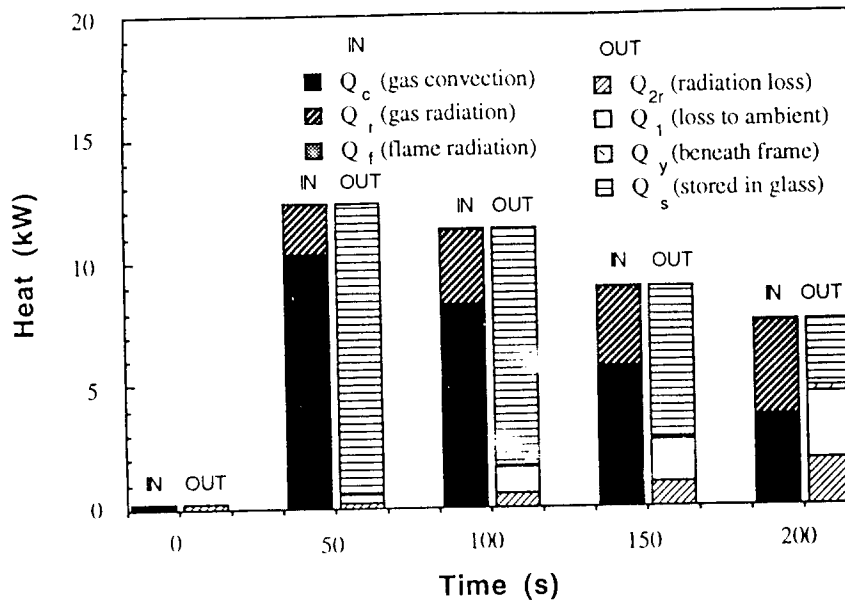


Fig. 9c. Predicted evolution of the magnitude of the various energy flow and storage terms for the University of California at Berkeley Richmond Field Station experiment shown in Figs 9a and 9b. This fire was quenched in the first minute by lack of oxygen.

emissivity of the hot gas layer, ϵ_{2x} , were estimated using data from glass breaking⁹ and backdraft¹⁰ experiments. A linear history for the heat transfer coefficient inside the fire compartment and a linear history for the emissivity of the hot layer gave good agreement with experimental glass temperatures.

ACKNOWLEDGMENTS

This work was supported by the Building and Fire Research Laboratory at the United States National Institute of Standards and Technology under Grant No. 60NANB80848. The authors would also like to thank I. Finnie, C. M. Fleischmann and M. Prime.

REFERENCES

1. Pagni, P. J. & Joshi, A. A., Glass breaking in fires. In *Fire Safety Science—Proc. 3rd Int. Symp.*, ed. G. Cox & B. Longford. Hemisphere, Washington, DC, 1991, p. 791.
2. Mitler, H. E. & Rockett, J. A., User's guide to FIRST, a comprehensive

- single-room fire model. Report No. 87-3595, US Department of Commerce, National Institute of Standards and Technology, Gaithersberg, MD, 1987, p. 124.
3. Bartenev, G. M., *The Structure and Mechanical Properties of Inorganic Glasses*. Wolters-Noordhoff Publishing, Groningen, The Netherlands, 1970.
 4. Finnie, I., Chapter 8 of class notes for ME 225, Fracture Mechanics of Engineering Materials. University of California at Berkeley, CA, 1991.
 5. Matthewson, M. J., An investigation of the statistics of fracture. In *Strength of Inorganic Glasses*, ed. C. R. Kurkjian. Plenum Press, New York, 1985, pp. 429-42.
 6. Weibull, W., A statistical distribution of wide applicability. *J. Appl. Mechanics*, **18** (1951) 293.
 7. Popov, I., *Introduction to the Mechanics of Solids*. Prentice-Hall, New York, 1979.
 8. Clark, C. E., *An Introduction to Statistics*. John Wiley, New York, 1953.
 9. Skelly, M. J., Roby, R. J. & Beyler, C. L., Window breakage in compartment fires, *J. Fire Protection Engg*, **3** (1991) 25.
 10. Fleichmann, C. M., Pagni, P. J. & Williamson, R. B., Exploratory backdraft experiments. *Fire Technology* (in press).
 11. Joshi, A. A. & Pagni, P. J., User's guide to BREAK1, the Berkeley algorithm for glass breaking in compartment fires. Report No. NIST-GCR-91-596, National Institute of Standards and Technology, Gaithersburg, MD, 1991.
 12. For further information contact Nippon Electric Glass Company Ltd, Des Plaines, IL 60018, USA.